Growth of Cr_2O_3 whiskers by the vapour–liquid–solid mechanism

SHINOBU HASHIMOTO, AKIRA YAMAGUCHI
Department of Materials Science and Engineering, Nagoya Institute of Technology, Gokiso-cho, Showa-ku, Nagoya, 466 Japan

When a powder mixture composed of Cr_2O_3, Al_2O_3, SiO_2 and C was placed on a graphite powder in an alumina crucible with a lid, and the crucible was set in an electric furnace and heated to $> 1350\,^{\circ}C$, Cr_2O_3 whiskers grew at the surface of the powder mixture. The microstructure in the powder mixture, thermal analysis of the powder mixture during heating, and whisker droplet were investigated. The whiskers were found to have grown by the vapour–liquid–solid (VLS) mechanism.

1. Introduction

Ceramic whiskers are grown by vapour or liquid phase reaction. The growth of vapour phase reactions are VLS [1] and VS [2] mechanisms. Morphologically, ceramic whiskers which are grown by the VLS mechanism [2–11] have droplets on their tops, and the whiskers are considered to have grown from them. However, Patrick *et al.* [12] reported that the droplet intercepted the growth of the whisker.

When a powder mixture composed of Cr_2O_3, Al_2O_3, SiO_2 and C was placed on a graphite powder in an alumina crucible with a lid, and the crucible was heated, Cr_2O_3 whiskers having droplets on their tops grew on the surface of the powder mixture. The effects of starting powder composition, temperature and time on the features of Cr_2O_3 whiskers grown were investigated. The growth mechanism of Cr_2O_3 whiskers was established.

2. Experimental procedure

The starting powder materials were reagent grade Cr_2O_3 (average grain size, 0.5 μm), Al_2O_3 (average grain size, 2.3 μm), SiO_2 ($\leqslant$ 35 μm) and C (graphite powder). Each of the powder mixtures, with various ratios of Cr_2O_3, Al_2O_3, SiO_2 (in total, 80 wt %) and C (20 wt %), were placed on graphite powder in an alumina crucible, as shown in Fig. 1a. The crucibles, with lids, were set in an electric furnace and heated at a rate of $600\,^{\circ}C\,h^{-1}$ at various temperatures for various times.

The growth of whiskers was observed by scanning electron microscopy (SEM), the component was identified by X-ray diffraction (XRD), and a droplet of a whisker was analysed by electron probe microanalysis (EPMA). The amount of solid solubility of Al_2O_3 in Cr_2O_3 was determined as follows. Dense sintered bodies with various compositions of Cr_2O_3 and Al_2O_3 were prepared [13]. A calibration curve between the relative intensity ratio of X-rays in EPMA and the weight fraction for Cr_2O_3 and Al_2O_3 mixing ratio was constructed. The amount of solid solubility of Al_2O_3 in the Cr_2O_3 whisker was determined from this calibration curve.

As shown in Fig. 2, the temperature of the powder mixture during heating was measured by a thermocouple which was set through a hole (measuring 1 × 10 mm) at the centre of the alumina lid into the powder mixture directly. The setting places were at the middle of the powder mixture (point b) and near the graphite powder in the powder mixture (point c) compared with the temperature in the furnace (point a). Moreover, the powder mixture after heating was embedded in epoxy resin and polished. The polished surface was analysed by EPMA.

3. Results

3.1. Features of the growing whiskers

Fig. 1b shows a schematic drawing of the cross-section of the alumina crucible after heating. Cr_2O_3 whiskers grew on the surface of the powder mixture. Fig. 3 shows the amount of whiskers grown by heating at $1400\,^{\circ}C$ for 4 h for various original compositions. The maximum amount of whiskers grown was obtained from an original composition of 40 wt % Cr_2O_3, 20 wt % Al_2O_3, 20 wt % SiO_2 and 20 wt % C. The composition was selected in the following experiments. Fig. 4 shows SEM photographs of the whiskers grown by heating at $1400\,^{\circ}C$ for 4 h. They had droplets on their surfaces.

3.2. Analysis of the whiskers

XRD patterns, Fig. 5, show that the grown whiskers were Cr_2O_3 crystals. Fig. 6 shows EPMA photographs of the droplet at the top of the whisker. Si, O and small Cr were detected. Al was detected in the Cr_2O_3 whisker, but not in the droplet. The amount of solid solubility of Al_2O_3 in the Cr_2O_3 whisker was determined at < 1 wt %.

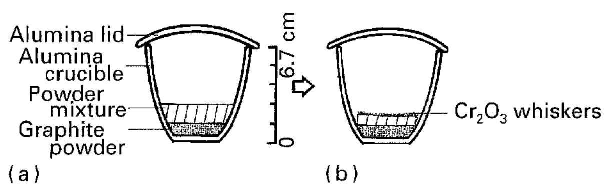

Figure 1 Schematic drawing of the crucible in which Cr_2O_3 whiskers were formed: (a) before heating, and (b) after heating.

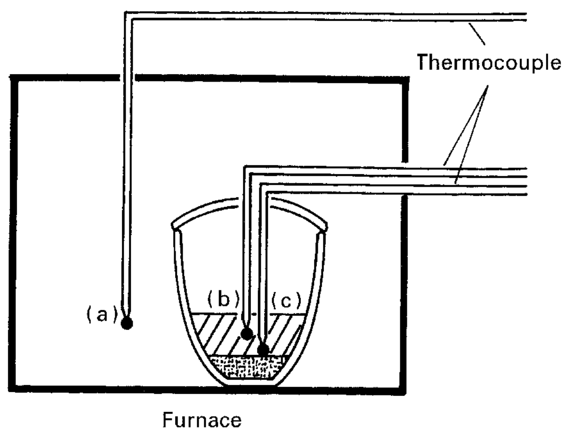

Figure 2 Schematic drawing of temperature measurement of the powder mixture during heating: (a) in the furnace, (b) in the middle of the powder mixture, and (c) near the graphite powder.

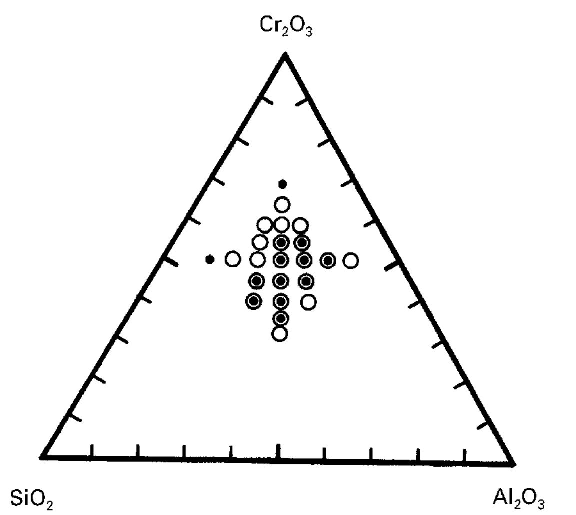

Figure 3 The amount of Cr_2O_3 whiskers grown by heating at 1400 °C for 4 h for various original compositions: (⊙) large, (○) small, (●) none.

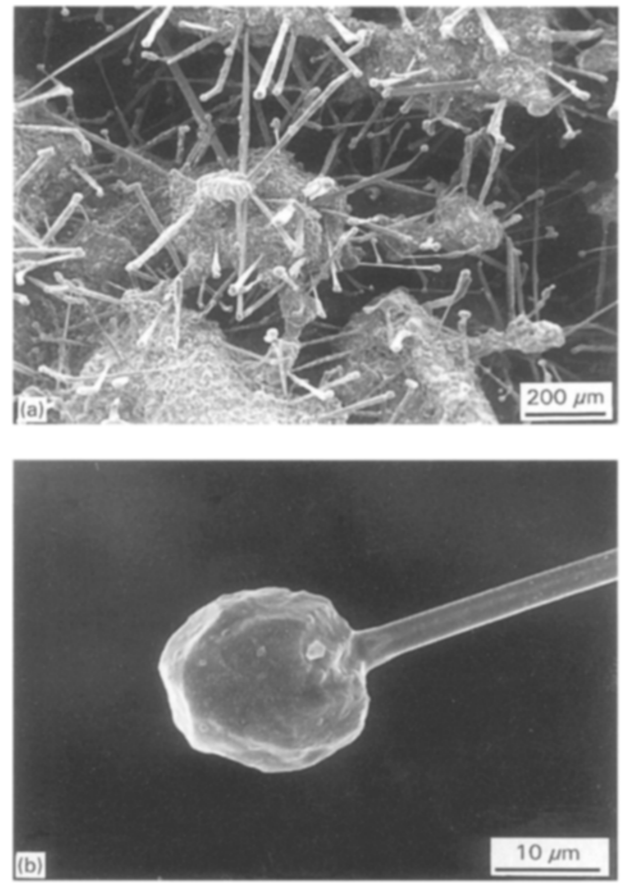

Figure 4 SEM photographs of the whiskers grown at 1400 °C for 4 h.

3.3. Effects of temperature and time on the growth of the whiskers

Fig. 7 shows change of average width and length with temperature at 1350–1450 °C for 4 h. On average, length and width of the whiskers grown by heating at 1390 °C for 4 h were about 1200 μm and 6.8 μm, respectively. Above 1390 °C, the powder mixture, remarkably, became a porous surface, and the amount of whiskers grown decreased. However, the width of the whiskers increased with temperature. Fig. 8 shows the change of average width and length of whiskers with time at 1400 °C. After the whiskers had grown to about 7 μm in diameter and 600 μm in length, growth seems to have stopped.

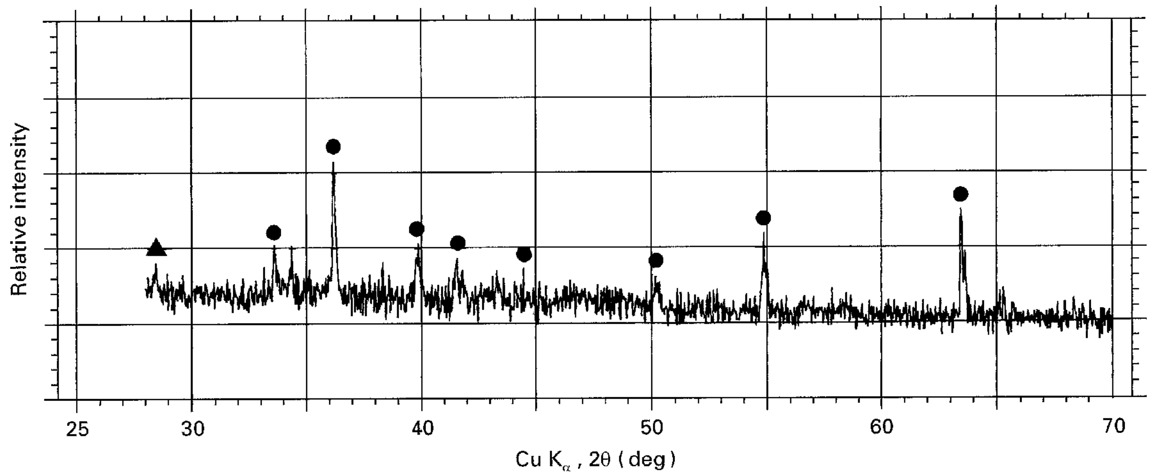

Figure 5 XRD pattern of the grown whiskers: (●) $Cr_2O_{3(solid)}$, (▲) $SiO_{2(solid)}$.

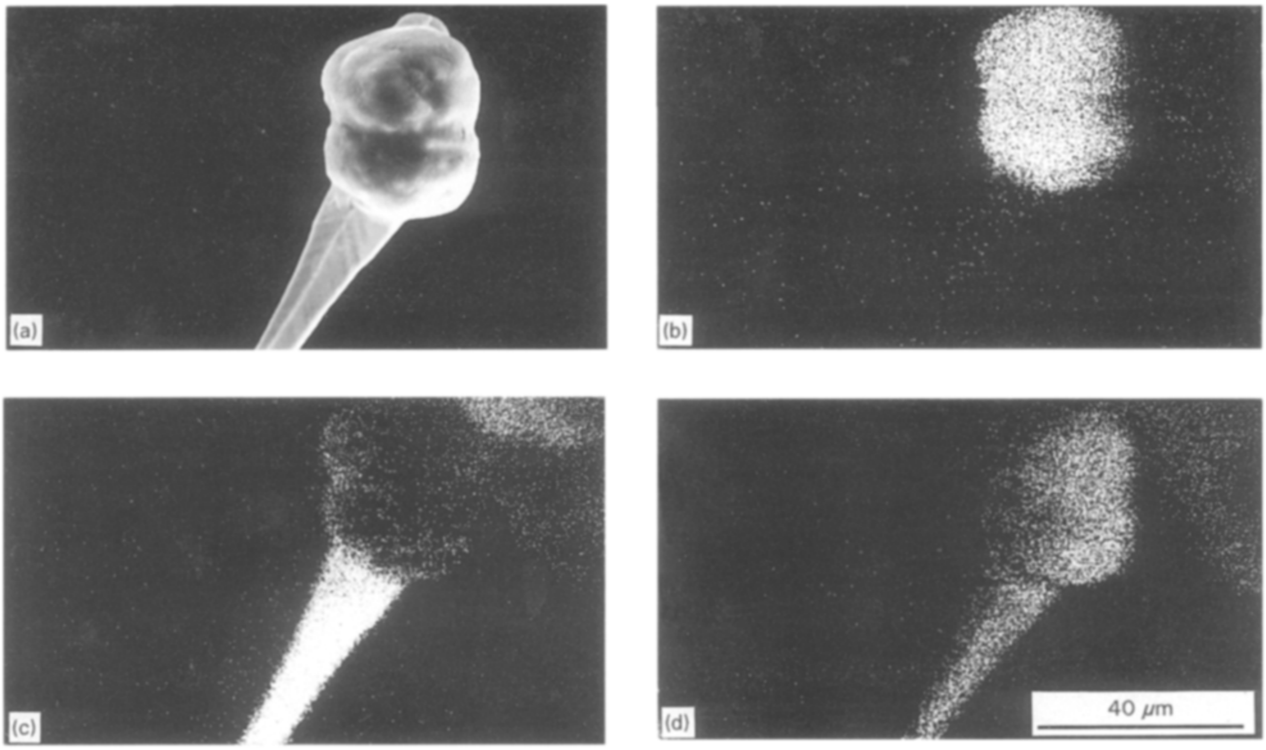

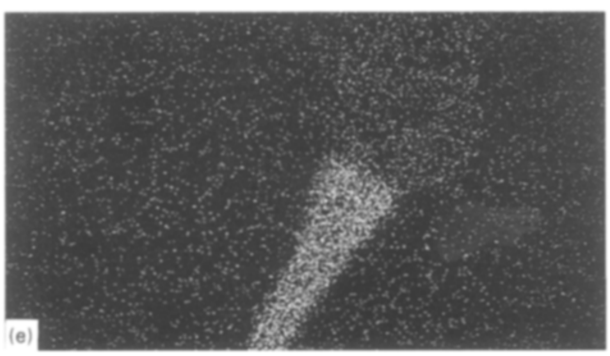

Figure 6 (a) SEM and EPMA photographs of K_α images of (b) Si, (c) Cr, (d) O, and (e) Al for the droplet at the top of a Cr_2O_3 whisker.

3.4. Behaviour of the powder mixture during heating

Fig. 9 shows the temperatures at points b and c, compared them to that of the furnace at point a in Fig. 2. At points b and c, the rising rate of the temperatures changed at approximately 1370 and 1290 °C, respectively. Fig. 10 shows a cross-section of the powder mixture heated at 1400 °C for a moment. Large pores were formed near the graphite powder. The powder mixture altered to Cr_2O_3–Al_2O_3 solid solution (s.s.), SiO_2 (cristobalite), small Cr_2O_3 and Cr_3C_2 after heating at 1400 °C for 4 h and was embedded in epoxy resin and polished. Fig. 11 shows EPMA photographs of the polished surface. Since Al, Cr and O were detected at the surface of the powder mixture, Cr_2O_3–Al_2O_3 (s.s.) existed, on which Cr_2O_3 whiskers were grown. The same reactants were present in the powder mixture after heating for 1 and 8 h. About 20–32 wt % Al_2O_3 was contained in Cr_2O_3–Al_2O_3 s.s.

4. Discussion

4.1. Behaviour of the powder mixture during heating

Liquid phase is not formed below 1575 °C in the Al_2O_3–Cr_2O_3–SiO_2 phase diagram [14]. Since, at $\geqslant 1000$ °C, the atmosphere under existing carbon is about 0.1 MPa $CO_{(gas)}$ [15], the atmosphere in the alumina crucible with carbon can be considered to be 0.1 MPa $CO_{(gas)}$ at $\geqslant 1000$ °C. Fig. 12 shows the relationship between the partial pressures of gaseous species and the stable condensed phases for the partial pressure of $CO_{(gas)}$ ($\log p_{CO}$) and the partial pressure of $O_{2(gas)}$ ($\log p_{O_2}$) in the system Si–Cr–Al–C–O at 1427 °C (1700 K) on the basis of JANA thermodynamics-data [16]. As an example, Cr_2O_3 is not a stable condensed phase at $-1 = \log p_{CO}$. At p_{CO}, vaporization of the oxides increased and the liquid phase can be generated at relatively lower temperature [17]. In fact, changes of rising rate of temperatures at

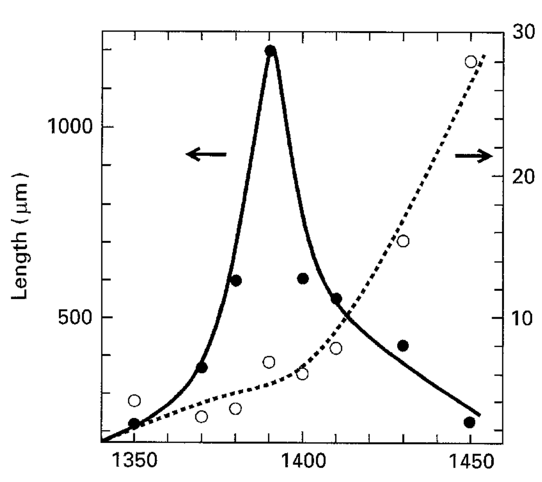

Figure 7 Changes of average length (●) and width (○) of Cr_2O_3 whiskers with temperature after 4 h.

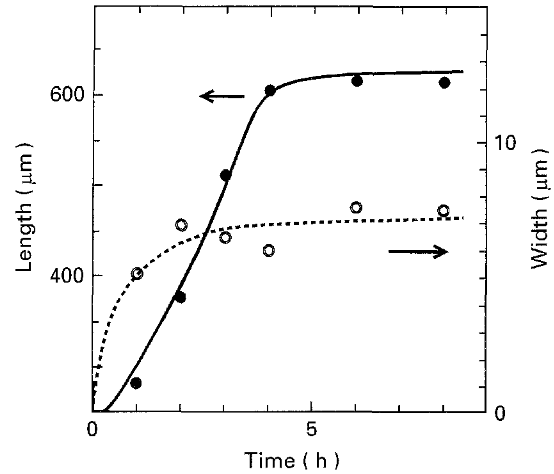

Figure 8 Changes of average length (●) and width (○) of Cr_2O_3 whiskers with time at 1400 °C.

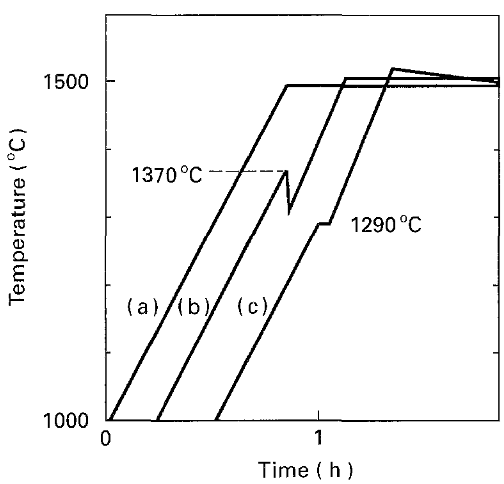

Figure 9 Changes of temperatures in the powder mixture under conditions of a constant heating rate of $600\,^{\circ}\mathrm{C\,h^{-1}}$: (a) in the electric furnace, (b) in the middle of the powder mixture, and (c) in the powder mixture near the graphite powder.

about 1290 and 1370 °C as shown, in Fig. 9, are considered to be responsible for the formation of the liquid phase.

As shown in Fig. 10, some large pores which are found near the graphite powder are due to be formed by generation of $CO_{(gas)}$ on the basis of Equation 1.

$$3Cr_2O_{3\,(solid)} + 13C_{(solid)} = 2Cr_3C_{2\,(solid)} + 9CO_{(gas)} \quad (1)$$

Since a $\log p_{CO}$, on the basis of Equation 1 at 1427 °C, is calculated at 0.66 ($p_{CO} = 4.60$ MPa) and the value is 46 times as large as atmospheric pressure, $CO_{(gas)}$ comes to be continuously exhausted out of the powder mixture during heating.

Other gaseous species generated from the powder mixture during heating can be considered as follows. $\mathrm{Log}\, p_{CO}$ in the powder mixture at 1427 °C seems to always change at − 1–0.66, at which Cr_2O_3 can condense, in Fig. 12. Then, $\log p_{SiO}$ is the highest among the gaseous species in Si–O system and the value is − 4.28 (point a in Fig. 12) to − 5.95 (point b). $\mathrm{Log}\, p_{Cr}$ is the highest value among the gaseous species in the Cr–O

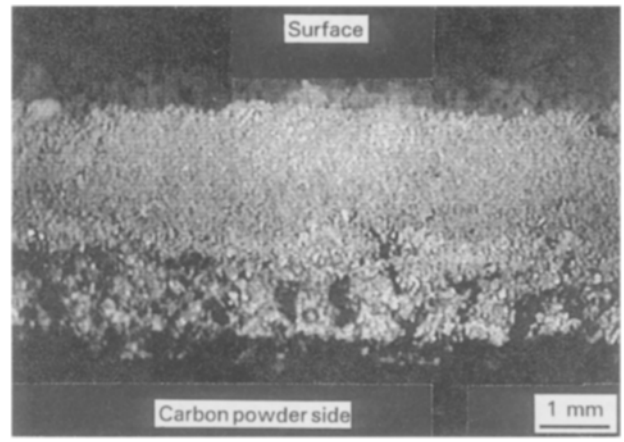

Figure 10 Cross-section of the powder mixture heated at 1400 °C for a moment.

system and the value is − 6.79 (point c–d). On the other hand, $\log p_{Al}$ which is the highest in the Al–O system is about a third to a sixth of $\log p_{Cr}$; in effect, negligible. After all, $SiO_{(gas)}$ and $Cr_{(gas)}$ are mainly exhausted from the powder mixture. A schematic drawing, Fig. 13a, shows the supplying process of the gaseous species from the powder mixture.

4.2. Growth mechanism of Cr_2O_3 whiskers

Cr_2O_3 whiskers are considered to be grown by the VLS mechanism because of the presence of droplets on the whisker surface, as shown in Fig. 4. Since Si, O and small Cr are detected at the droplet, as shown in Fig. 6, the droplet is reflected to be Si–Cr–O liquid during heating. That is, the liquid is developed by the formation of SiO_{2-x}–Cr_2O_{3-y} at lower p_{O_2}. $SiO_{(gas)}$ and $Cr_{(gas)}$ carry out efficiently to the surface of the powder mixture with exhausting $CO_{(gas)}$, and condense as a liquid of Si–Cr–O. $SiO_{(gas)}$ and $Cr_{(gas)}$ further dissolve in the liquid. The supersaturation of Cr_2O_3 which is caused by dissolving $O_{2\,(gas)}$, precipitates Cr_2O_3 crystals at the bottom of the liquid. The process is repeated to form the whisker with a droplet on its top. Fig. 13b shows a schematic drawing of the Cr_2O_3 whisker grown by the VLS mechanism in this study.

When the powder mixture composed of Cr_2O_3, SiO_2, and C was used, Cr_2O_3 whiskers did not grow. It is considered that Al_2O_3 decreases the melting point of the powder mixture and accelerates the occurrence of the liquid phase. Therefore, p_{CO} is higher in the powder mixture and the exhausting $CO_{(gas)}$ then accelerates the supplying of $SiO_{(gas)}$ and $Cr_{(gas)}$ for the growth of Cr_2O_3 whiskers at lower temperatures.

4.3. Effect of temperature and time on the growth of Cr_2O_3 whiskers

The lengths of Cr_2O_3 whiskers decrease with temperature after showing a maximum value around 1390 °C as shown in Fig. 7. Fig. 14 shows the equilibrium partial pressures of $SiO_{(gas)}$ and $Cr_{(gas)}$ under the existence of (SiO_2 + C) and (Cr_3C_2 + C) at 0.1 MPa $CO_{(gas)}$, respectively. At about 1390 °C, the values of p_{SiO} and p_{Cr} may be suitable for the growth of whiskers. Since the

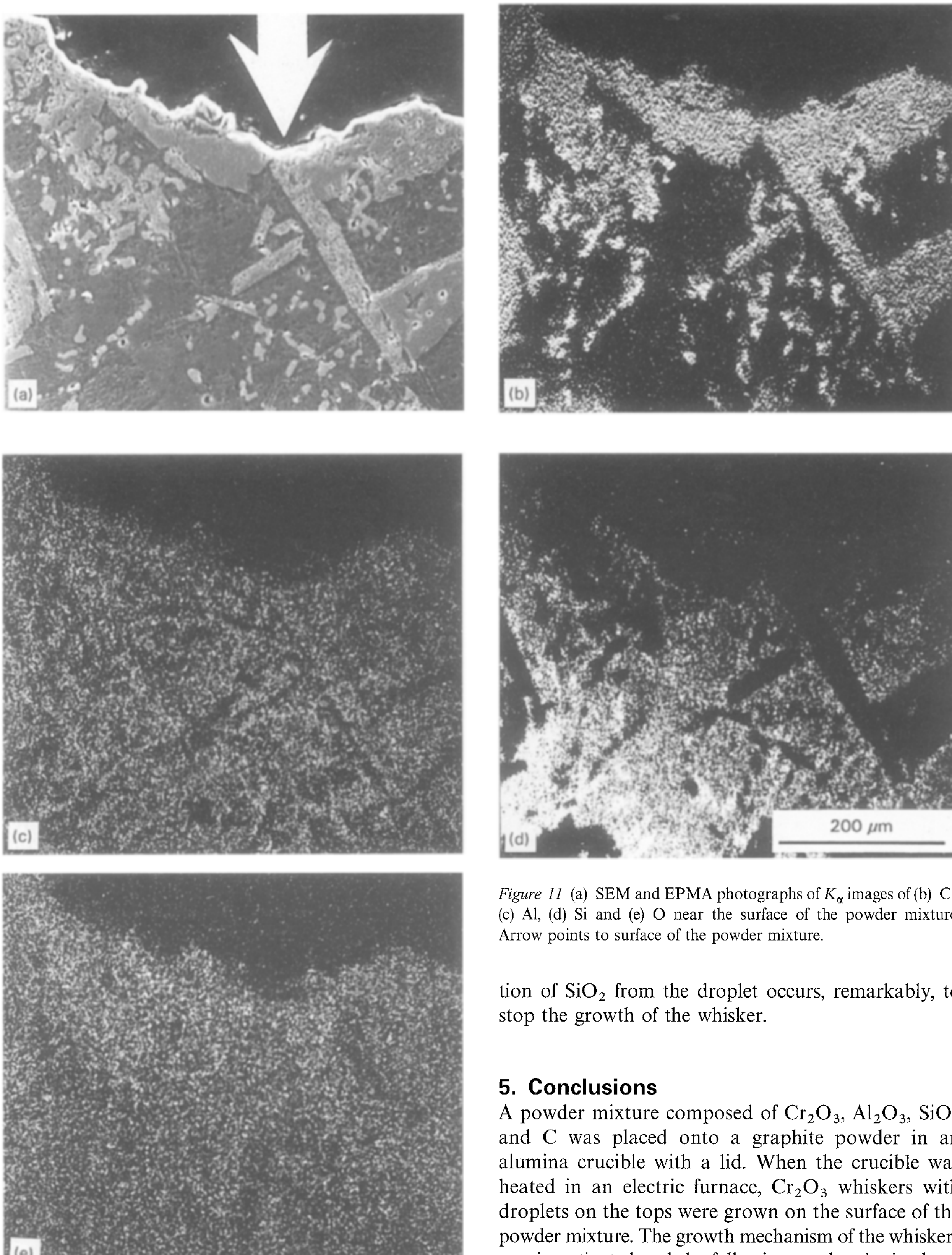

Figure 11 (a) SEM and EPMA photographs of K_α images of (b) Cr, (c) Al, (d) Si and (e) O near the surface of the powder mixture. Arrow points to surface of the powder mixture.

rate of increase of log p_{SiO} is larger than that of log p_{Cr} with temperature, the SiO_2/Cr_2O_3 ratio in the droplet is considered to increase. As a result, SiO_2 can precipitate from the droplet to intercept the growth in the elongated direction of the whisker. On the other hand, the growth in width of the whiskers with temperature is due to the VS mechanism [2] acting at the lateral surfaces of the whiskers. At $> 1450\,°C$, the precipitation of SiO_2 from the droplet occurs, remarkably, to stop the growth of the whisker.

5. Conclusions

A powder mixture composed of Cr_2O_3, Al_2O_3, SiO_2 and C was placed onto a graphite powder in an alumina crucible with a lid. When the crucible was heated in an electric furnace, Cr_2O_3 whiskers with droplets on the tops were grown on the surface of the powder mixture. The growth mechanism of the whiskers was investigated and the following results obtained.

1. Si–Cr–O liquid in the powder mixture is formed at $> 1290\,°C$. $SiO_{(gas)}$ and $Cr_{(gas)}$ are mainly supplied by exhausting $CO_{(gas)}$ which is generated by reaction of Cr_2O_3 and C.

2. Cr_2O_3 whiskers are grown by the VLS mechanism. The whisker is grown from a droplet that is generated by condensation of $SiO_{(gas)}$ and $Cr_{(gas)}$ and is a liquid of Si–Cr–O at growing temperatures.

3. The average width and length of the whiskers grown by heating the powder mixture composed of 40 wt % Cr_2O_3, 20 wt % Al_2O_3, 20 wt % SiO_2 and

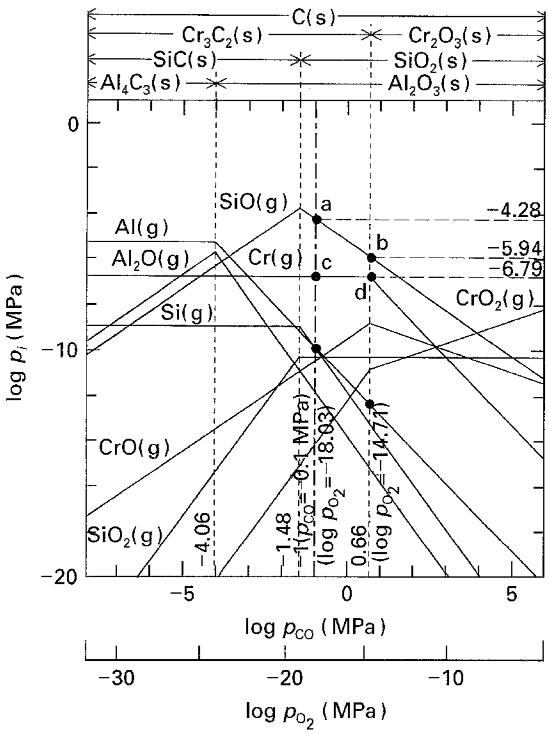

Figure 12 Relationship between the partial pressures of gaseous species and stable condensed phases for $\log p_{O_2}$ and $\log p_{CO}$ in the system Si–Cr–Al–C–O at 1427 °C. Points a and b show the $\log p_{SiO}$ at -1 and $0.66 = \log p_{CO}$, respectively. Points c and d show the $\log p_{Cr}$ at -1 and $0.66 = \log p_{CO}$, respectively. No marked two points show the $\log p_{Al}$ at -1 and $0.66 = \log p_{CO}$.

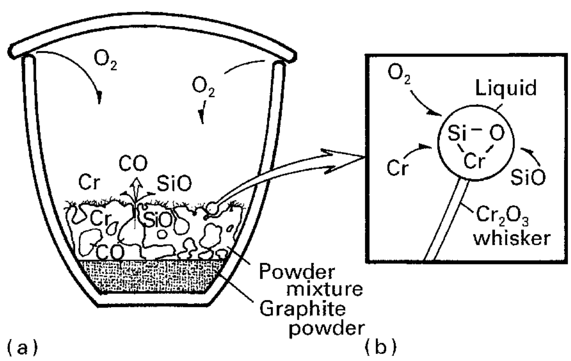

Figure 13 Schematic drawing explaining growth mechanism of Cr_2O_3 whiskers: (a) gaseous species exhausting from the powder mixture during heating, and (b) VLS mechanism of a Cr_2O_3 whisker.

20 wt % C at 1390 °C for 4 h are about 6.8 and 1200 μm, respectively. The width of the whiskers is increased and the length decreased with temperature at above 1390 °C. The whiskers are not grown above 1450 °C.

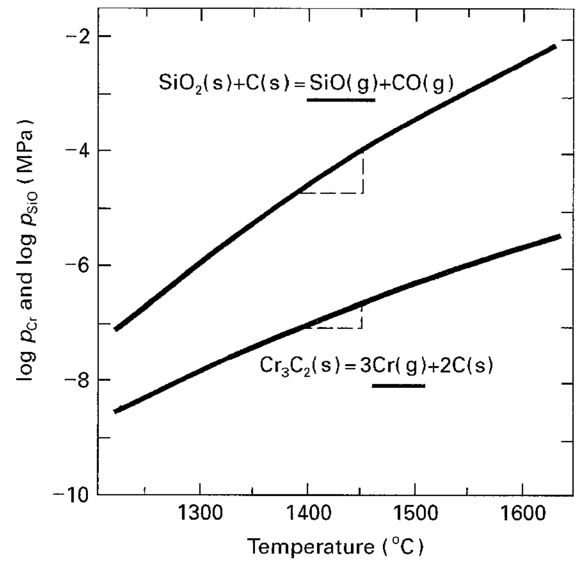

Figure 14 Equlibrium partial pressures of $SiO_{(gas)}$ and $Cr_{(gas)}$ under existence (SiO_2–C) and (Cr_3C_2–C) at 0.1 MPa $CO_{(gas)}$, respectively.

References

1. R. S. WAGNER and W. S. ELLIS, *Trans. Met. Soc. AIME* **233** (1965) 1503.
2. A. KATO and N. TAMARI, *J. Cryst. Growth* **49** (1980) 199.
3. A. H. HEUER and P. BURNETT, *J. Amer. Ceram. Soc.* **50** (1967) 627.
4. M. SCHREINER, W. WRUSS and B. LUX, *J. Cryst. Growth* **61** (1983) 75.
5. K. SUGIYAMA, Y. TAKAHASHI and S. MOTOJIMA, *Chem. Lett.* **37** (1975) 363.
6. T. HAYASHI, S. KAWABE and H. SAITO, *Yogyo-Kyoukai-Shi* **94** (1986) 19.
7. N. SETAKA and C. KAWASHIMA, *J. Ceram. Assoc. Jpn* **76** (1968) 154.
8. W. E. HOLLAR Jr and J. J. KIM, *Ceram. Eng. Sci. Proc.* **12** (1991) 979.
9. N. HOLONYAK Jr, C. M. WOLF and J. S. MOORE, *Appl. Phys. Lett.* **6** (1965) 64.
10. R. L. BARNS and W. C. ELLIS, *J. Appl. Phys.* **36** (1965) 2296.
11. S. MANSOUR and R. SCHOLZ, *Mater. Lett.* **9** (1990) 511.
12. L. PATRICK, D. R. HAMILTON and W. J. CHOYKE, *Phys. Rev.* **143** (1966) 526.
13. A. YAMAGUCHI, *Yogyo-Kyoukai-Shi* **90** (1982) 68.
14. P. L. ROEDER, F. P. GLASSER and E. F. OSBORN, *J. Amer. Ceram. Soc.* **51** (1968) 585.
15. A. YAMAGUCHI, *Taikabutsu* **38** (1986) 232.
16. M. W. CHASE Jr *et al.*, *J. Phys. Chem. Ref. Data* **14** (1985) Supplement 1.
17. A. YAMAGUCHI, *Ceram. Int.* **12** (1986) 19.

Received 15 February
and accepted 17 July 1995